The Journal of The Textile Institute

ISSN: 0040-5000 (Print) 1754-2340 (Online) Journal homepage: https://www.tandfonline.com/loi/tjti20

Analysis and prediction of woven compression bandages properties

Abdelhamid Rajab Ramadan Aboalasaad & Brigita Kolčavová Sirková

To cite this article: Abdelhamid Rajab Ramadan Aboalasaad & Brigita Kolčavová Sirková (2019) Analysis and prediction of woven compression bandages properties, The Journal of The Textile Institute, 110:7, 1085-1091, DOI: 10.1080/00405000.2018.1540284

To link to this article: https://doi.org/10.1080/00405000.2018.1540284

Published online: 21 Nov 2018.

THE JOURNAL OF THE TEXTILE INSTITUTE
2019, VOL. 110, NO. 7, 1085–1091
https://doi.org/10.1080/00405000.2018.1540284

Analysis and prediction of woven compression bandages properties

Abdelhamid Rajab Ramadan Aboalasaad and Brigita Kolčavová Sirková

Department of Textile Technologies, Technical University of Liberec, Liberec, Czechia

ABSTRACT

Compression bandage (CB) as a porous material consists of elastic textile that exerts pressure on muscles. Three common types of woven CBs are evaluated. Uniaxial stresses of the input yarns and the produced bandage will be tested. This work presents a new method to predict optimum required tension when applying CB on lower leg ankle and mid-calf positions. Experimental measurements and data analysis using NIS software enable to analyze and calculate the bandage porosity during extension using high speed camera. Practical bandage pressure is measured using PicoPress tester. The obtained results will be compared with theoretical compression forces calculated by a modified Laplace's law equation which predicts graduated compression ranging from 27 to 72 mmHg at the ankle, tapering to 18–8 mmHg below the knee. Results confirm that theoretical pressure is not exactly consistent with practical compression.

ARTICLE HISTORY
Received 12 October 2017
Accepted 19 October 2018

KEYWORDS
Bandage structures; tension; porosity; Laplace's law; PicoPress

1. Introduction

Medical compression bandages (MCBs) are widely used in the treatment of venous leg ulcers. In order to design effective compression bandages (CBs), researchers have attempted to describe the interface pressure applied by these bandages using mathematical models (Al Khaburi, Dehghani-Sanij, Nelson, & Hutchinson, 2012; Rimaud, Convert, & Calmels, 2014; Schuren & Mohr, 2008).

Venous ulceration is the most common type of leg ulceration and a significant health problem, affecting approximately 1% of the population and 3% of people over 80 years of age in westernized countries (Franks et al., 2016). Systematic reviews and meta-analyses have identified good quality evidence from randomized controlled trials (RCTs) to support the use of advanced or antimicrobial dressings (such as iodine, honey or silver dressings) for chronic wounds (Williams, 2016).

In clinical practice, bandages are applied in the form of overlapping layers which results in multiple layers of fabric that overlay a particular point of the surface of the limb (Al Khaburi, Dehghani-Sanij, Nelson, & Hutchinson, 2011). For example, MCBs applied with spiral 50% overlap technique will overlay the leg with two layers of bandage, MCBs applied with 66% overlap will result in three layers of bandage and MCBs applied with the figure-of-eight technique with 50% overlap will result in four layers of bandage (Al Khaburi et al., 2012; Rimaud et al., 2014).

MCBs aim to provide graduated compression to the lower limb from the ankle to the knee in order to improve venous return, accelerate venous flow, reduce venous reflux by realignment of valves, improve venous pump action, and to reduce edema (Fletcher, Moffatt, Partsch, Vowden, & Vowden, 2013; Halfaoui & Chemani, 2016). In order to design effective compression systems, improve practice and help nurses or patients to achieve the optimum gradient pressure, many researchers have attempted to describe or predict the sub-bandage interface pressure theoretically (Al Khaburi, Nelson, Hutchinson, & Dehghani-Sanij, 2011; Sikka, Ghosh, & Mukhopadhyay, 2016; Thomas, 2003). Most of the studies reported in the literature have focused on the investigation of some physical and mechanical properties of one-directional stretch fabrics. However, there is paucity of literature on bi-stretch fabrics comprising elastane containing core-spun cotton yarns both in the warp and weft directions. Maqsood investigated the effect of elastane linear density, fabric thread density, and weave float size on the fabric contraction, sub-bandage pressure, fabric stretch, and recovery properties of bi-stretch woven fabrics for compression garments (Maqsood, Hussain, Malik, & Nawab, 2016).

Hence, it was necessary to evaluate the structure of three basic types of woven CBs showing the material, production as well as deformation viewpoint during the uniaxial stress. Then introduce a new method to predict suitable CB tension by measuring the bandage porosity using high speed camera. The obtained results are compared with theoretical compression forces calculated by a modified Laplace's law equation as follows (Chemani & Halfaoui, 2014; Maqsood, Nawab, Umar, Umair, & Shaker, 2017; Partsch, & Mortimer, 2015):

$$\text{Pressure (Pa)} = \frac{\text{Tension (N)} \times \text{Number of layers}}{\text{Radius (m)} \times \text{Bandage width (m)}} \quad (1)$$

The level of pressure exerted from a medical device answers to the Laplace equation stating that the pressure (P expressed in Pa) of a compression applied to the skin surface is proportional to the tension (T in N) of the

CONTACT Abdelhamid Rajab Ramadan Aboalasaad eabdo6@gmail.com

			
Cotton/Polyamide/ Polyurethane	Bleached Cotton	Viscose-Lycra	Viscose-Polyamide
C-PA-PU	100 % Cotton	94% Viscose, 6 % Lycra	56% Viscose, 44% Polyamide

Figure 1. Woven compression bandages characteristics.

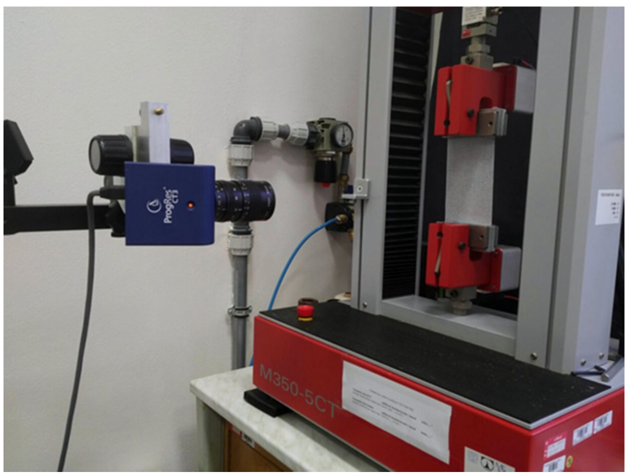

Figure 2. Testometric M350-5CT instrument adjustment with high speed camera.

compression material and number of layers, and inversely proportional to the radius of curvature (R in m) of limb surface to which it is applied and the bandage width (w in m) (Kumar, Das, & Alagirusamy, 2013a; Rimaud et al., 2014).

There are two types of practical pressure (i.e. static and dynamic pressure). Static pressure is the permanent pressure a compression means exerts to tissue and vessels while the musculature is relaxed. The resulting power to apply or stretch a CB is equal to the power which is affected to the tissue as static pressure. Therefore, static pressure is often described as the applied pressure. Dynamic (operating) pressure occurs when the muscle acts against the resistance of the compression means, because its volume increases through contraction. This way, the operating pressure is generated and is therefore described as muscle pressure (Kumar, Das, & Alagirusamy, 2013b; Rotsch, Oschatz, Schwabe, Weiser, & Möhring, 2011).

2. Experimental work

2.1. Materials

a. Four basic types of woven CBs (Cotton/Polyamide/ Polyurethane, 100% Cotton, Viscose-Lycra, and Viscose-Polyamide bandages as shown in Figure 1) are evaluated. These bandages structure is plain weave. Yarn counts and densities are different depends on the construction and technology of the final product.
b. Two groups of warp yarns were kept in a conditioning room for 24 h at standard temperature ($20 \pm 2\,^{\circ}C$) and relative humidity (65%) before testing. The tested warp yarns characteristics can be summarized in Tables 1 and 2.

2.2. Testing procedure

1. Load–elongation curve of the yarns is measured according to test method ISO 2062:2009(E) (ISO, 2009). Instron 4411 tensile testing machine was used to measure the tension developed in the yarn while extension at a constant speed of 180 mm/min. A 100 N load cell was used to measure the bandage tension. The device gauge length was set to 500 mm.
2. CBs tension is evaluated according to test method ISO 13934-1:1999(E) (ISO E., 1999). Testometric M350-5CT was used to measure the tension developed in the bandage while extension at a constant speed of 100 mm/min. A 100 N load cell was used to measure the tension in the bandage. The device gauge length was set to 100 mm.
3. Bandage porosity is calculated by measuring the binary area fraction during different bandage extension using high speed camera as shown in Figures 2, 9, 10.
4. Bandages pressure was measured for all the bandage samples using PicoPress as shown in Figure 3 (Jariyapunya, Kholiavko, & Musilová, 2017; Kwon, et al., 2018). The obtained results are both digital numbers and graph forms. There are three levels of bandage tension (low: 50% extension and 50% overlap, medium: 100% extension and 50% overlap, and high: 100% extension and 66% overlap) applied on 1st position (ankle at radius 3.9 cm), 2nd (mid-calf at radius 6.2 cm), and 3rd (below the knee at radius 4.9 cm).

Table 1 Yarn properties (group 1: plied yarns, single yarn 6 tex).

Yarn twist (T/m)	Yarn count (tex)	Tenacity (cN/tex)	SD of tenacity	Extension (%)	SD of extension
300	11.78	23.64	1.4275	4.75	0.6118
600	12.16	24.86	1.5201	5.14	0.6515
900	12.87	23.51	1.9156	6.44	0.8210
1200	13.24	20	1.7504	6.98	0.7502
1500	13.71	18.09	1.4808	7.67	0.6346
1800	13.96	16.49	1.5827	8.21	0.6783

Table 2 Yarn properties (group 2: plied yarns, single yarns 25 and 40 tex respectively).

Yarn twist (T/m)	Yarn count (tex)	Tenacity (cN/tex)	SD of tenacity	Extension (%)	SD of extension
1850	49.37	15.53	1.2982	12.01	0.6491
2100	50.15	12.85	1.2596	12.19	0.6298
2200	74.72	9.86	1.4965	15.78	0.7483
2300	85.27	8.52	1.2289	15.77	0.6144

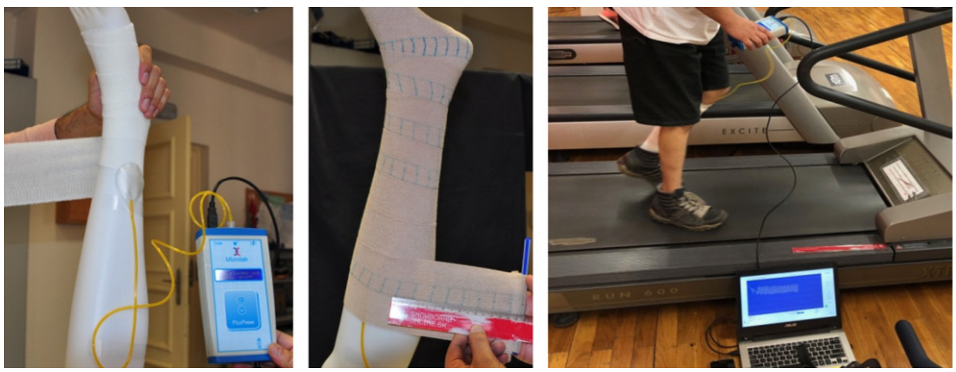

Figure 3. Microlab PicoPress instrument M-700 and its results.

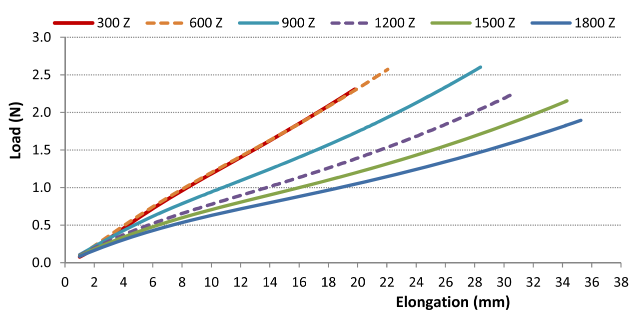

Figure 4. Load–elongation curves of the 1st group yarns.

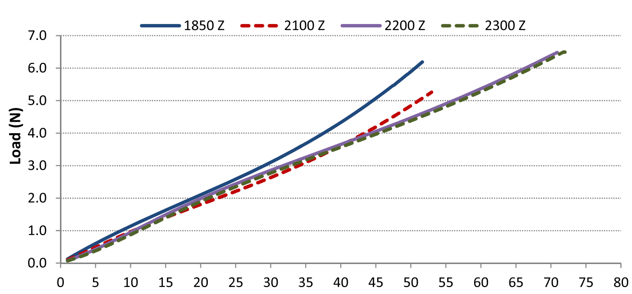

Figure 5. Load–elongation curves of the 2nd group yarns.

3. Results and discussion

3.1. Load–elongation curve of the yarns

A Matlab code was prepared to calculate the average load elongation curve for each twist (using raw data for 50 samples for each twist). For comparison between yarns the program interpolates the elongation data using equal step (0.05 mm) before the break point and gives the corresponding load values.

Figure 4 illustrates that increasing the plied yarn twist from 300 to 900 turns/m increases the breaking load and elongation by a percent ranges 12.8 and 43.4% respectively. After that the yarns breaking load is proportionally decreasing by increasing the yarn twist from 900 to 1800 turns/m. On the contrary the yarns elongation is increasing.

Whereas the plied yarns at twist 2100 turns/m is giving less tension values than 1850 turns/m, then the load increased by a percent 23.4% at 2300 turns/m. Moreover the yarn extension is proportionally increasing when the yarn twist increased from 1850 to 2300 turns/m by a percent 39.43%, as shown in Figure 5.

The obtained results in Figures 3 and 4 are giving some remarks to select the optimum yarn twist, but it's not enough because the twist range and the yarns count are different. At least (1500–1800 turns/m) are required for producing high extension cotton CBs, whereas to achieve 100% elastic cotton CB (2200–2300 turns/m) would be used.

3.2. Relation between yarn twist and tenacity

Taking into consideration the yarn properties; the comparison would be using the tenacity and strain (extension %) of the yarns.

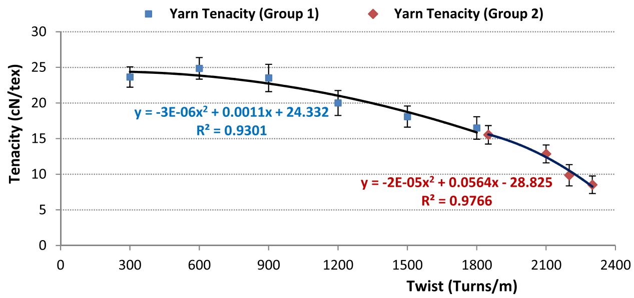

Figure 6. Effect of yarn twist on its tenacity.

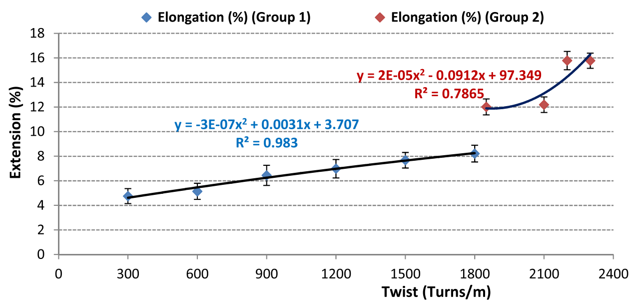

Figure 7. Effect of yarn twist on its extension.

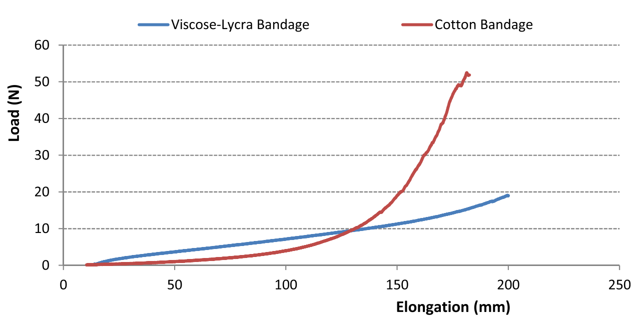

Figure 8. Load–elongation curves of Viscose-Lycra and Cotton bandages.

$$\text{Tenacity} = \text{Breaking load (N)} \times 100/\text{Yarn count (tex)} \quad (2)$$

$$\text{Strain} = \Delta L/L_1 \text{ or extension}(\%) = \Delta L \times 100/L_1 \quad (3)$$

$$\Delta L = L_2 - L_1 \quad (4)$$

where L_2 is the extended length of yarn, L_1 is the initial (gauge) length.

These yarn parameters can be displayed as shown in Figures 6 and 7 to give clear comparison and good selection of the optimum yarn twist. The candidate results of yarn tenacity and breaking elongation wouldn't be reached when producing the elastic CB because these bandages are only produced using the elastic region of the yarns. The 1st group of plied yarns is giving higher tenacity values than the 2nd group but lower elongation (%). So the best selection of the yarn twist and count depends on the end use of the CB.

3.3. Load–elongation curve of the bandages

Load–elongation curves for both Cotton and Viscose-Lycra bandages were analyzed as shown in Figure 8. Bandage samples were subjected to 200% extension of its original length. Both Cotton and Viscose-Lycra bandages required tension of 10 N at 130% extension; these values are achieving the required bandage pressure (4000 Pa or 30 mmHg) according to Laplace's law equation (1) for two layers bandaging at radius 5 cm and bandage width 10 cm. For pressure more than 30 (mmHg): Viscose-Lycra bandages have more extension than Cotton bandages, (i.e. Viscose-Lycra bandages can be stretched 200% using load 20 N, whereas Cotton bandages are stretchable to 180% only then it will break at point 52 N).

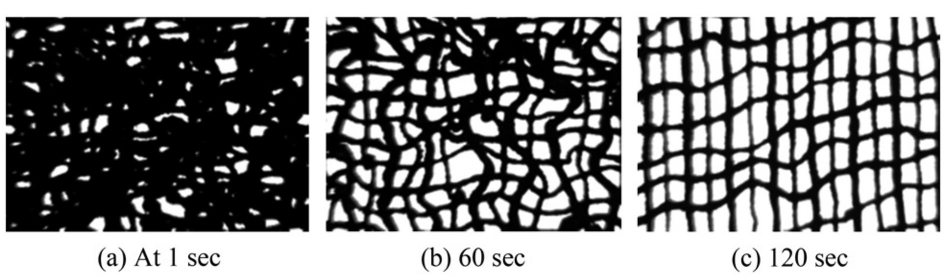

Figure 9. Binary area of Cotton bandage during tension.

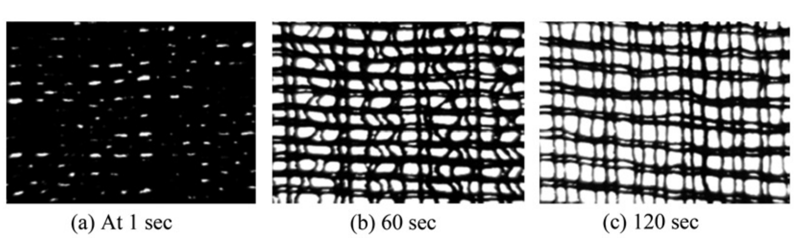

Figure 10. Binary area of Viscose-Lycra bandage during tension.

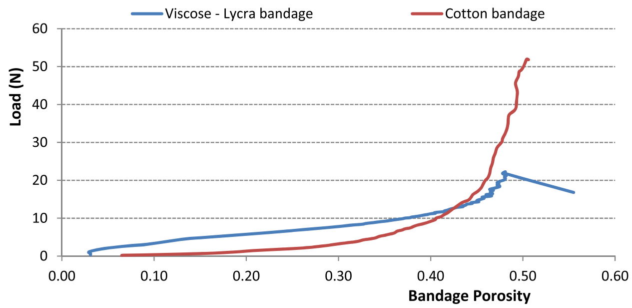

Figure 11. Effect of applied tension on bandage porosity.

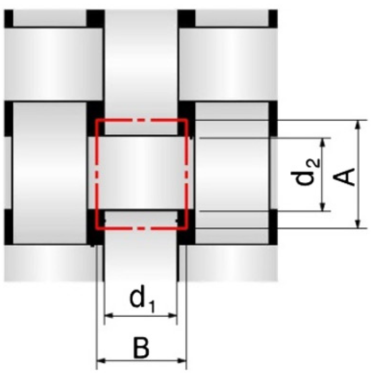

Figure 12. Structure of interlacing cell in woven fabric crossing point of plain weave, warp and weft diameter (d_1, d_2), warp and weft spacing (*B*, *A*).

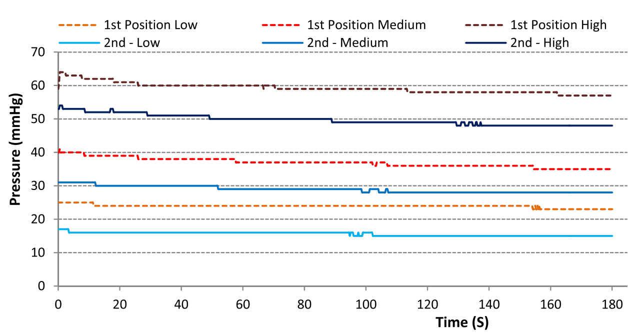

Figure 13. Pressure of Cotton bandage on leg model.

3.4. Effect of applied tension on bandage porosity

While subjecting the bandage samples to constant extension, the resultant images were recorded using high speed camera as shown in Figures 9 and 10. There are 120 frames (images) for each sample; these images were analyzed to measure bandage porosity as a function of binary area fraction using Threshold technique during loading and extension as shown in Figure 11.

3.5 Relation between bandage porosity and applied tension

Figure 11 illustrates the relation between binary area fraction – which represents the bandage porosity – and the applied tension. Taking the fabric thickness into consideration, "*Fabric porosity is defined as the volume of voids among fibers*" (Abo-Taleb, El-Fowaty, & Sakr, 2015; Havlová, 2014; Neckar & Das, 2012).

$$\text{Porosity} = V_P/V_T \tag{5}$$

where V_P is the volume of air pores (cm^3), V_T is the total volume of the sample (cm^3).

If we deal with two dimensional fabric, porosity is defined as the ratio of the projected geometrical area of the opening across the material to the total area of the material (Cay, Atrav, & Duran, 2007; Hani et al., 2013). An area of pores is calculated as a perpendicular projection of the woven fabric (horizontal porosity). Real values can be measured as illustrated in Equation (6) (Elnashar, 2005):

$$Ps = 1- \ CF = 1-(d_o D_o + d_u D_u - d_o d_u D_o D_u) \tag{6}$$

where d_o, d_u are the diameters of warp and weft yarn respectively, and D_o, D_u are the sets of warp and weft yarns respectively.

According to the theory of 2-D model, the woven fabric porosity is defined as a complement to the woven fabric cover factor (CF), see Figure 12.

Cover factor can be calculated on the basic of illustrated structure of woven fabric as illustrated in Figure 12 by

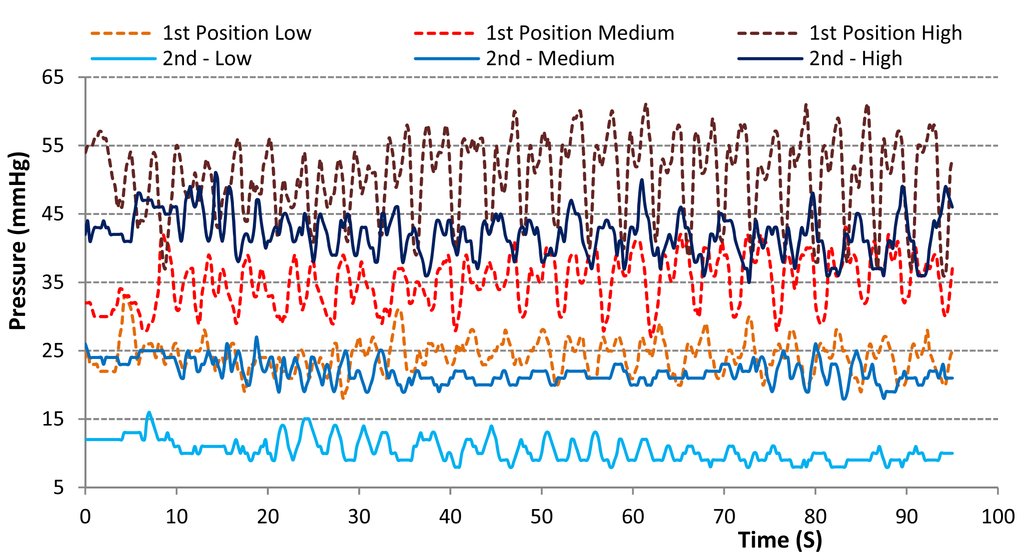

Figure 14. Pressure of Cotton bandage on real leg while walking.

Equation (7):

$$CF = \frac{\text{visible area covered by yarns}}{\text{totalareaofcell}} = \frac{d_1A + d_2B - d_1d_2}{AB} = CF_{warp} + CF_{weft} - CF_{warp}CF_{weft} \quad (7)$$

Based on known parameters of the warp and weft density (D_1 and D_2) respectively, Equation (8) could be derived as following:

$$A = \frac{1}{D_2} \text{and } B = \frac{1}{D_1} \quad (8)$$

3.6. Testing of bandage pressure using PicoPress

Experimental pressures of CBs (100% Cotton and Viscose-Lycra) are measured using PicoPress on mannequin leg as shown in Figure 13. The same compression test for all types of bandages on real leg at 1st, 2nd and 3rd positions as shown in Figures 14–17. First type of bandages is 100% cotton using highly twisted plied cotton yarns. Average compression values at 1st position for the three tension levels (low, medium, high) were about (24, 37, 59 mmHg). All 1st position results are decreasing by average percent 12% after 180 s, whereas for 2nd position compression values were (16, 29, 50 mmHg) decreasing by average percent 11%. This decrease may be due to bandage slippage and less fixation on leg model.

As for applying CBs on a real leg; all compression tests were applied on the same group of 4 men, their age ranges 28–37 years old. Figure 14 emphasizes the significant change of compression during walking, which is oscillating between (18–33, 27–43 and 36–61 mmHg) for 1st position, (8–16, 18–27 and 35–51) for 2nd position. These oscillations during walking and running should be considered while wearing the CBs for long time to achieve effective healing rates. Figure 15 shows the pressure of C-PA-PU CB while walking; that is ranging (10–19, 20–35 and 34–50 mmHg) for 1st position, (17–23, 22–26 and 27–37 mmHg) for 2nd position and (12–15, 13–18 and 13–19 mmHg) for 3rd position. Oscillating ranges of C-PA-PU bandage are less than for high twist Cotton bandage because of more extensibility.

While Viscose-Lycra CB introduced less oscillating pressure range i.e. (14–19, 26–30 and 46–56 mmHg) for 1st position and (12–16, 17–22 and 32–45) for 2nd position, as illustrated in Figure 16. This low range of pressure is due to Lycra extensibility. Moreover the Viscose-Polyamide bandages are giving the lowest compression pressure values compare to other types; this may be due to yarns characteristics and type of heat setting to give the stretch and extensibility of the bandages, this type of bandage is more suitable for hand muscles, see Figure 17.

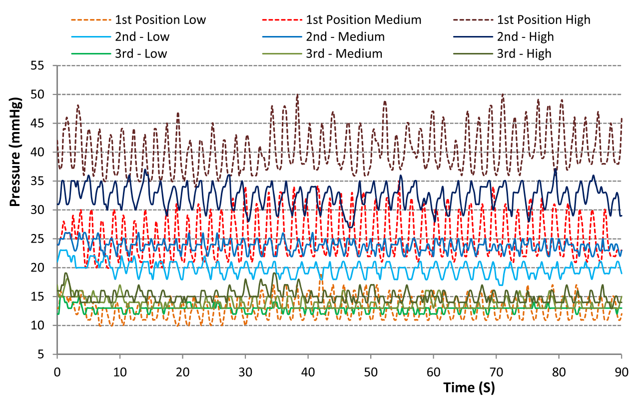

Figure 15. Pressure of C-PA-PU bandage on real leg while walking.

4. Conclusion

Candidate work presented a new method to predict bandage tension as a function of bandage extension; that enables the patient to use the bandage himself more easily. The experimental compression results were compared with theoretical pressure calculated by Laplace's law equation. Statistical analysis confirmed that there are significant differences between theoretical pressure and practical compression results.

PicoPress results confirmed that 100% Cotton bandages achieved the highest pressure ranges i.e. (18–33, 27–43 and

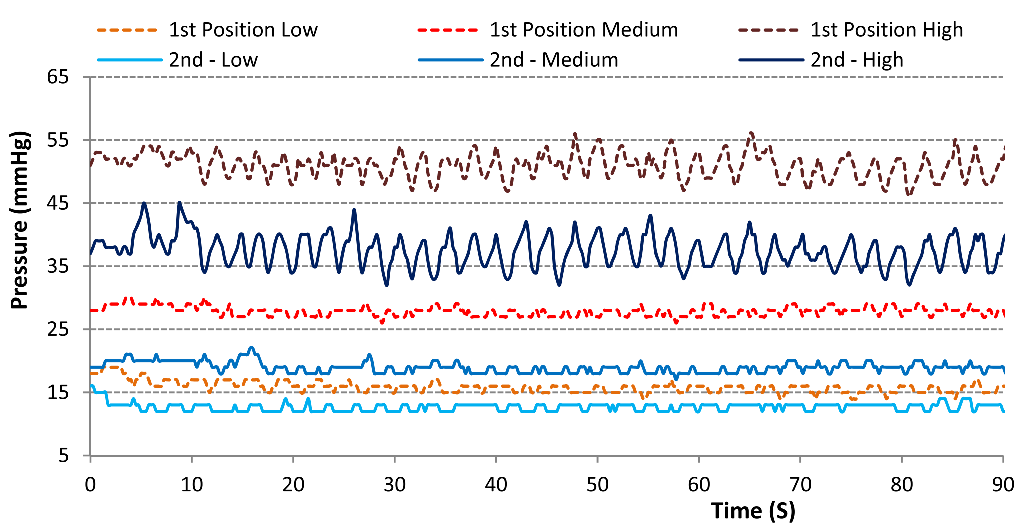

Figure 16. Pressure of Viscose-Lycra bandage on real leg while walking.

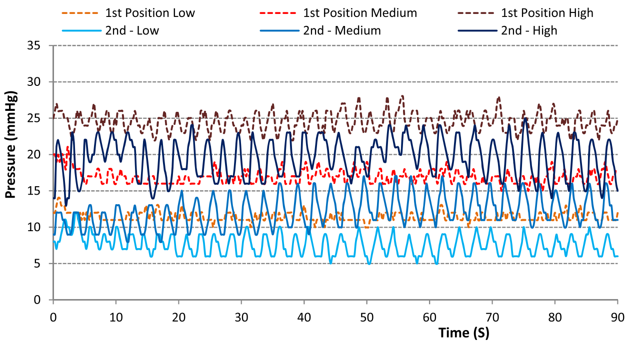

Figure 17. Pressure of Viscose-Polyamide bandage on real leg while walking.

36–61 mmHg) for 1st position, (8–16, 18–27 and 35–51) for 2nd position. The best selection of bandage type and optimum gradual pressure decreasing at the ankle through the calf to the knee, depends on the type of patient disease, age and suitable healing rate. The higher oscillating ranges of practical pressure may be due to applying these bandages on a little group of men having varied ages and strength; these oscillating ranges may be decreased when applying the bandages for a large group of patients at the same conditions.

Disclosure statement

No potential conflict of interest was reported by the authors.

Funding

This work is supported under Student Grant Scheme (SGS 21196) by Technical University of Liberec, Czech Republic.

References

Abo-Taleb, H., El-Fowaty, H., & Sakr, A. (2015). Theoretical prediction of overall porosity of terry woven fabrics. *Journal of Textile Science & Engineering*, *5*(6), 1.

Al Khaburi, J., Dehghani-Sanij, A. A., Nelson, E. A., & Hutchinson, J. (2011). The effect of multi-layer bandage on the interface pressure applied by compression bandages. *World Academy of Science, Engineering and Technology, International Journal of Mechanical, Aerospace, Industrial, Mechatronic and Manufacturing Engineering*, *6*, 1169–1174.

Al Khaburi, J., Dehghani-Sanij, A., Nelson, A., & Hutchinson, J. (2012). Effect of bandage thickness on interface pressure applied by compression bandages. *Medical Engineering & Physics*, *34*(3), 378–385.

Al Khaburi, J., Nelson, E. A., Hutchinson, J., & Dehghani-Sanij, A. A. (2011). Impact of multilayered compression bandages on sub-bandage interface pressure: A model. *Phlebology: The Journal of Venous Disease*, *26*(2), 75–83.

Cay, A., Atrav, R., & Duran, K. (2007). Effects of warp-weft density variation and fabric porosity of the cotton fabrics on their colour in reactive dyeing. *Fibres & Textiles in Eastern Europe*, *1*(60), 91–94.

Chemani, B., & Halfaoui, R. (2014). Influence of pressure from compression textile bands: Their using in the treatment of venous human leg ulcers. *World Academy of Science, Engineering and Technology, International Journal of Chemical, Molecular, Nuclear, Materials and Metallurgical Engineering*, *8*(8), 812–817.

Elnashar, E. A. (2005). Volume porosity and permeability in double-layer woven fabrics. *AUTEX Research Journal*, *5*(4), 207–217.

Fletcher, J., Moffatt, C., Partsch, H., Vowden, K., & Vowden, P. (2013). Principles of compression in venous disease: a practitioner's guide to treatment and prevention of venous leg ulcers. *Wounds International*, 1–21. Retrieved from www.woundsinternational.com

Franks, P. J., Barker, J., Collier, M., Gethin, G., Haesler, E., Jawien, A., & … Weller, C. (2016). Management of patients with venous leg ulcers: Challenges and current best practice. *Journal of Wound Care*, *25*(Sup6), S1–S67.

Hani, A., Shaari, M., Radzuan, N., Hashim, M., Ahmad, R., & Mariatti, M. (2013). Analysis of woven natural fiber fabrics prepared using self-designed handloom. *International Journal of Automotive and Mechanical Engineering*. *8*, 1197–1206. ISSN: 2180-1606 (Online).

Halfaoui, R., & Chemani, B. (2016). New approach to predict pressure produced by elastic textile in the therepeutic treatment of venous leg. *Journal of Fundamental and Applied Sciences*, *8*(2), 297–312.

Havlová, M. (2014). Model of vertical porosity occurring in woven fabrics and its effect on air permeability. *Fibres & Textiles in Eastern Europe*, *22* (4), 58–63.

ISO. (2009). E. 2062. Textiles – Yarns from packages – Determination of single-end breaking force and elongation at break using constant rate of extension (CRE) tester (ISO 2062: 2009) ICS 59.080. 20 ISO. TC, 38.

ISO E. (1999). Textiles – Tensile properties of fabrics – Part 1: Determination of maximum force and elongation at maximum force using the strip method. No. EN ISO, 13934-1.

Jariyapunya, N., Kholiavko, N., & Musilová, B. (2017). *Designing method for 3D modeling for garment compression values of elastic fabric extension* (Ph. D. Students Day, 44).

Kumar, B., Das, A., & Alagirusamy, R. (2013a). An approach to examine dynamic behavior of medical compression bandage. *Journal of the Textile Institute*, *104*(5), 521–529.

Kumar, B., Das, A., & Alagirusamy, R. (2013b). Study on interface pressure generated by a bandage using in vitro pressure measurement system. *The Journal of the Textile Institute*, *104*(12), 1374–1383.

Kwon, C., Hegarty, M., Oxenham, W., Thoney-Barletta, K., Grant, E., & Reid, L. (2018). An indirect testing approach for characterizing pressure profiles of compression bandages and hosiery. *The Journal of the Textile Institute*, *109*(2), 256–267.

Maqsood, M., Hussain, T., Malik, M. H., & Nawab, Y. (2016). Modeling the effect of elastane linear density, fabric thread density, and weave float on the stretch, recovery, and compression properties of bi-stretch woven fabrics for compression garments. *The Journal of the Textile Institute*, *107*(3), 307–315.

Maqsood, M., Nawab, Y., Umar, J., Umair, M., & Shaker, K. (2017). Comparison of compression properties of stretchable knitted fabrics and bi-stretch woven fabrics for compression garments. *The Journal of the Textile Institute*, *108*(4), 522–527.

Neckar, B., & Das, D. (2012). *Theory of structure and mechanics of fibrous assemblies*. New Delhi: Woodhead Publishing India Pvt. Ltd.

Partsch, H., & Mortimer, P. (2015). Compression for leg wounds. *The British Journal of Dermatology*, *173*(2), 359–369.

Rimaud, D., Convert, R., & Calmels, P. (2014). In vivo measurement of compression bandage interface pressures: The first study. *Annals of Physical and Rehabilitation Medicine*, *57*(6–7), 394–408.

Rotsch, C., Oschatz, H., Schwabe, D., Weiser, M., & Möhring, U. (2011). Medical bandages and stockings with enhanced patient acceptance. In V. Bartels (Ed.), *Handbook of medical textiles* (pp. 481–504). UK: Woodhead Publishing Ltd.

Schuren, J., & Mohr, K. (2008). The efficacy of Laplace's equation in calculating bandage pressure in venous leg ulcers. *Wounds UK*, *4*(2), 38–42.

Sikka, M. P., Ghosh, S., & Mukhopadhyay, A. (2016). Mathematical modeling to predict the sub-bandage pressure on a conical limb for multi-layer bandaging. *Medical Engineering & Physics*, *38*(9), 917–921.

Thomas, S. (2003). The use of the Laplace equation in the calculation of sub-bandage pressure. *EWMA J*, *3*(1), 21–23.

Williams, A. (2016). A review of the evidence for adjustable compression wrap devices. *Journal of Wound Care*, *25*(5), 242–247.